

Synthesis and characterization of silica–silver core–shell composite particles with uniform thin silver layers

Shaochun Tang, Yuefeng Tang, Shaopeng Zhu, Haiming Lu, Xiangkang Meng*

Department of Materials Science and Engineering, National Laboratory of Solid State Microstructures, Nanjing University, Nanjing 210093, People's Republic of China

Received 19 May 2007; received in revised form 22 July 2007; accepted 20 August 2007
Available online 4 September 2007

Abstract

Silica–silver core–shell composite particles with uniform thin silver layers were successfully synthesized by a facile and one-step ultrasonic electrodeposition method. By electrolysis of the slurry consisting of preformed silica spheres and silver perchlorate without any additives, the homogenous composite particles can be prepared. The average size of single silver crystals in the composite is about 12 nm and the thickness of silver layer is 14 ± 2 nm. Moreover, the continuity of Ag distribution, the surface roughness and the thickness of silver layer are controllable by adjusting the current density (I), the concentration of electrolyte (C) and the reaction time (t). Optical properties of the composite particles with different silver content were also investigated.

© 2007 Elsevier Inc. All rights reserved.

Keywords: Thin silver layer; Ultrasonic electrodeposition method; Silica–silver composite particles; Optical properties

1. Introduction

In recent years, dielectric-metal core–shell building structures (nanoshells) represent a new type of constructional unit and have attracted much attention. These hybrid particles have greatly potential application in various fields such as surface-enhanced Raman scattering [1], modulation of optical properties [2], photonics [3], biological detection [4], magnetics [5], and catalysis [6], etc. Especially, mono-dispersive nanoshells are promising building blocks of photonic crystals (PCs) with large dielectric contrast, which has been demonstrated to have complete photonic band gap (CPBG) even in the optical wavelengths [7,8]. In general, this kind of core–shell structure was fabricated by depositing nanoscaled metal particles on dielectric spheres with various methods. Silver-coated silica nanoshells, for example, have been fabricated by a variety of approaches such as pretreatment of electroless deposition [9], seeding plating [10], polyol process [11], surface functionalization [12] and layer-by-

layer process [13]. However, it is relatively complex because these silica-coating procedures usually involved multistep processes and it is quite difficult to obtain a dense and uniform nanoscaled silver layer with high purity. In the synthesis of nanoshells, there are often some problems to be solved such as incomplete coverage, rough surfaces, nonuniformity in shell thickness, and poorly controlled composition [14]. Besides, present study focused on coating the silica spheres with dense and uniform silver layer in the thickness range of 20–100 nm, however, the uniform and complete coverage of each particle in a sample by a defined silver coating below 20 nm thick, which is the basis for several fundamental investigations involving optical phenomena, still remains a challenge. In addition, simplicity and controllability of the process are necessary for industrial applications. Therefore, further exploration and evaluation of deposition methods are necessary for the preparation of optically interesting materials.

In this paper, a facile and one-step ultrasonic electrodeposition method, which has recently been used for deposition of monodisperse Ag nanoparticles on silica substrate [15], is extended to entirely and evenly coat the surfaces of dielectric silica spheres with uniform thin silver

*Corresponding author. Fax: +86 25 8359 5535.

E-mail address: mengxk@nju.edu.cn (X. Meng).

layers. The resulted silver-coated silica nanoshells were demonstrated by X-ray diffraction (XRD), transmission electron microscopy (TEM), selected area electron diffraction (SAED), high-resolution transmission electron microscopy (HRTEM) and energy dispersive X-ray (EDX) microanalysis. The reaction parameters such as the current density (I), the concentration of electrolyte (C) and the reaction time (t) for the formation of uniform silver layers were studied. Optical properties of the composite particles with different silver content were also investigated.

2. Experimental

The silica spheres used as the substrates were prepared by the modified Stöber method [16]. Typically, 12 ml of ammonia solution was diluted by 64 ml of anhydrous ethanol in a conical flask and placed in a water bath at a constant temperature (35 °C). Then another mixture solution of 12 ml $\text{Si}(\text{OC}_2\text{H}_5)_4$ and 66 ml anhydrous ethanol was added to the conical flask drop by drop under vigorous magnetic stir. Gentle stir continued for 24 h to ensure that the reaction was complete. A milk suspension with silica spheres was then separated by means of centrifuging at 3000 rpm for 5 min, washed with deionized water and anhydrous ethanol for at least five times.

Subsequently, take these silica spheres as substrates to prepare Ag/SiO_2 composite particles, note that the silica spheres were used for silver deposition without any further treatment. Two identical silver slices (the effective surface area was $2\text{ cm} \times 2\text{ cm}$) were used as the anode and the cathode, respectively, which were 4 cm apart from each other. A quadrate insulating electrochemical cell consisting of two-electrode setup was put inside an ultrasonic cleaner with its volume of 2 l, in which there was 400 ml of water. A direct current power supply was an electrophoresis apparatus trophoresis that maintain a constant current or voltage. Electrolysis of the 40 ml of slurry consisting of silica submicrospheres (200–300 mg) and silver perchlorate ($3.25 \times 10^{-6}\text{ mol/l}$) was carried out with the current density of $2\text{ mA}/\text{cm}^2$ for 30 min under continuous ultrasonic radiation with the frequency of 40 kHz and the power of 50 W. The starting pH of the electrolyte solution was 9.01. Finally, the suspension was centrifuged at 3000 rpm for 5 min. The product was purified successively by five more centrifugation/rinsing/redispersion steps with deionized water and anhydrous ethanol and dried at 40 °C for 12 h in an oven.

XRD measurements were performed to investigate the crystallinity, the average crystal size and the crystal structure of silver in the resulted products. XRD patterns of the samples were measured with a D/Max-RA XRD (using $\text{CuK}_\alpha = 1.5418\text{ \AA}$ radiation). The size, distribution, and morphology of silver particles on silica spheres were studied by TEM) that was performed with a FEI TECNAI F20 microscope, operating at 200 kV accelerating voltage and equipped with an EDX detector. The elemental composition and structural analysis of the products were

analyzed by EDX, SAED and HRTEM, which were also performed with the same microscope. The UV–visible absorption spectroscopy was carried out on an America VARIAN CARY 50 Probe UV–visible spectrophotometer with wavelength in range of 300–800 nm.

3. Results and discussion

Fig. 1 displays the XRD pattern of the sample obtained when I , C and t were $2\text{ mA}/\text{cm}^2$, $3.25 \times 10^{-6}\text{ mol/l}$ and 30 min, respectively. Several main diffraction peaks are observed at 38.12° , 44.34° , 64.52° , 77.31° (2θ), which correspond to the (111), (200), (220) and (311) reflections of fcc phase silver (JCPDS card No 4-783). This result indicates the presence of silver in the sample and the good crystallinity of the silver product. The XRD peaks are relatively broad due to the small size of the nanocrystals. The FWHM of the peaks corresponding to (111), (200), (220) and (311) reflections are 0.61, 0.65, 0.68 and 0.70, respectively. According to the well-known Scherrer diffraction formula ($d = k\lambda/\beta \cos \theta$), the average single crystal size is calculated to be 12 nm (the FWHM datum of four reflections was all used in the Scherrer equation). A very broad XRD reflection peak at 22° (2θ) is also observed, which is attributed to the amorphous silica spheres.

Fig. 2a display a TEM image of as-prepared silica spheres, the individual silica substrates in these images are spherical in shape, with smooth edges and bare surface. The silica substrates have a narrow size distribution and an average diameter of the substrates are about 647 nm. Further details of the silver–silica nanocomposites, including the morphology, the size and the composition, can be obtained from TEM and HRTEM observations, which are shown in Figs. 2b–g with gradually increscent resolution of the sample analyzed in Fig. 1. The TEM image with a relatively low magnification (Fig. 2b), shows that the product is very homogeneous. It is observed that the silica spheres have been coated and the dispersive composite particles in these images remain spherical in shape with

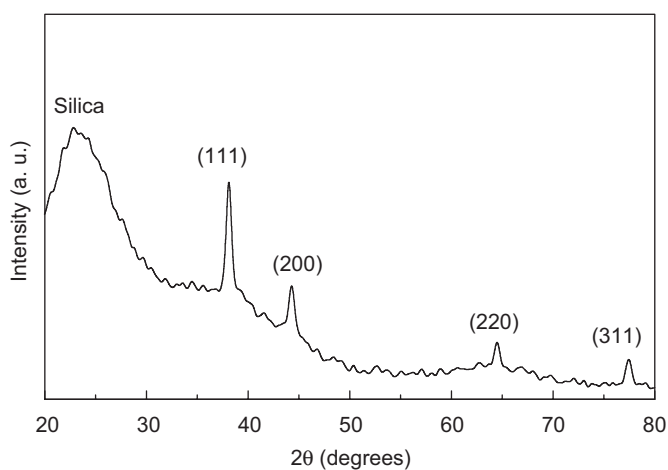


Fig. 1. XRD pattern of the sample synthesized when I , C and t were $2\text{ mA}/\text{cm}^2$, $3.25 \times 10^{-6}\text{ mol/l}$, and 30 min, respectively.

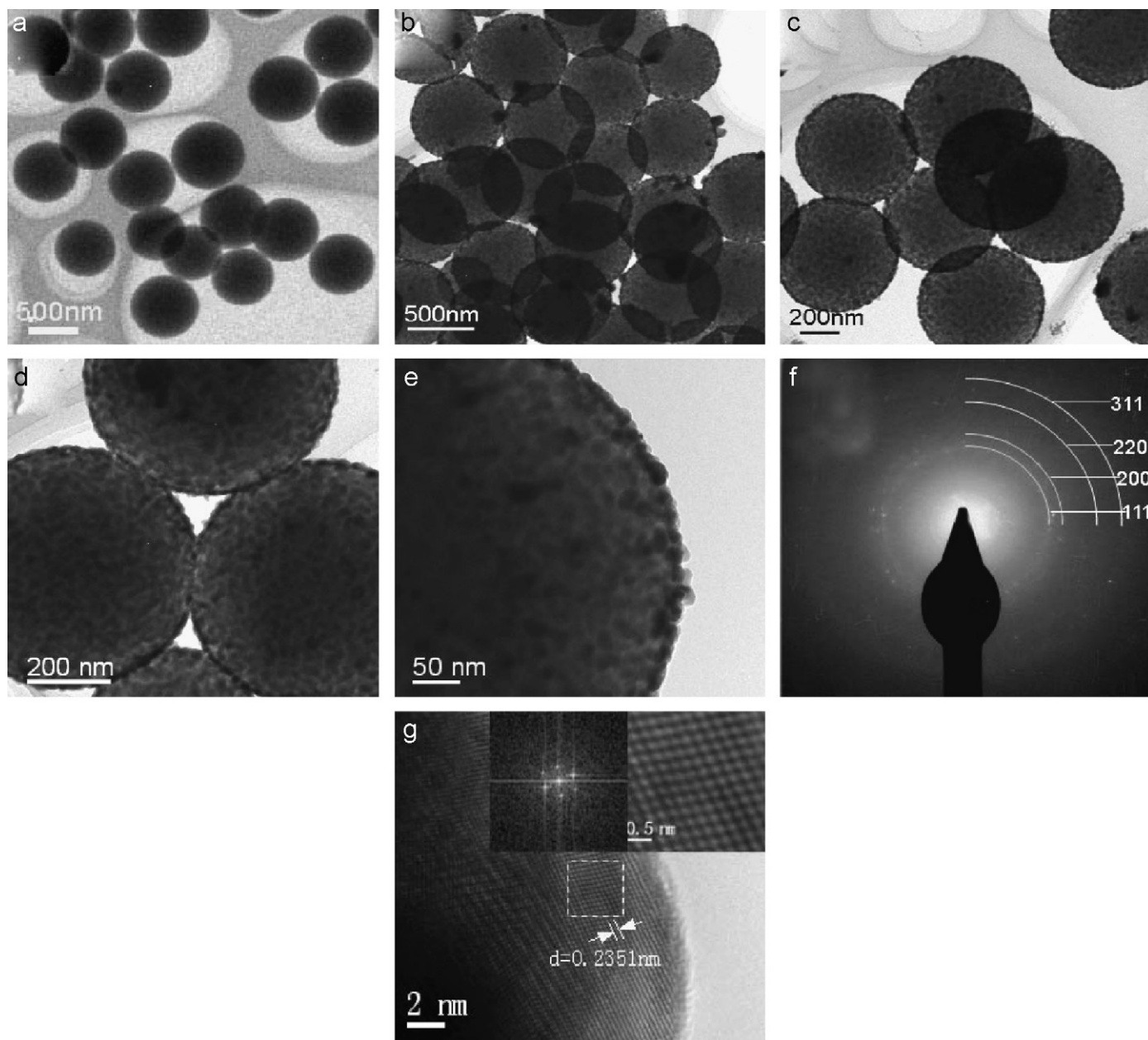


Fig. 2. (a) TEM image of the silica spheres before the coating; (b)–(e) TEM images with different magnifications; (f) SAED pattern of the entire SiO_2/Ag composite particle corresponding to (e); and (g) HRTEM image of the sample obtained when I , C and t were 2 mA/cm^2 , $3.25 \times 10^{-6} \text{ mol/l}$ and 30 min, respectively.

average diameter of 673 nm. TEM images with higher magnification shown as Figs. 2c–d indicate that silver nanocrystals are darker in contrast and distribute homogeneously and consecutively on the silica spheres. As observed in Fig. 2e, a single silica sphere has been completely covered by consecutive silver layer. The thickness of silver consecutive layer is measured to be $14 \pm 2 \text{ nm}$. The silver layer is deposited on the surface of the silica sphere by the ultrasonic electrodeposition process; therefore, it is composed of many silver nanoparticles. The continuously distributed silver particles cover the silica surface completely to form a silver shell due to their quite high filling factor on the silica surface. The corresponding

SAED pattern of an entire Ag/SiO_2 composite sphere displays several diffraction rings, which emanate from multiple nanocrystals on the surface of a silica sphere, as shown in Fig. 2f. The d spaces between lattice planes are calculated to be respectively 0.2360, 0.2037, 0.1441 and 0.1230 nm, corresponding to (111), (200), (220) and (311) planes of fcc structural silver (JCPDS No. 4-783). A HRTEM image shown in Fig. 2g indicates high crystallinity of silver in the product. The lattice space is measured to be 0.2351 nm, which is close to that of (111) planes for fcc silver (0.2359 nm). The insets in the right upper corner of Fig. 2g are, respectively, local magnification image of the selected section of the square and computer-generated fast

Fourier transform diffraction pattern, which also confirm the fcc structure of silver nanocrystals.

Fig. 3 shows the pattern of EDX measurements of the coated silica spheres with silver layers of 14 ± 2 nm. EDX analysis displays strong Si, O and Ag peaks next to Cu and C peaks and no other impurities can be detected. Note that the existence of Cu and C results from the sample support. High purity of silver nanocrystals can be confirmed by the results. Moreover, a table as an inset in the upper right corner in Fig. 3 shows the weight and atomic percentages of every detected element, according to the quantification results, a quantitative estimate of the Ag/Si atomic percentage ratio is about 1:4.

Therefore, it can be concluded from the above results that a highly pure, uniform and consecutive silver nanocoating on silica spheres can be obtained at the appropriate reaction by this electrodeposition procedure under ultrasonic conditions. Furthermore, this method is controllable and by adjusting the experimental conditions, such as I , C and t , dispersive silver nanoparticles or silver layers with different surface roughness and different thickness can also be obtained.

For example, as we have recently reported that when I , C and t were 0.75 mA/cm^2 , $3.25 \times 10^{-7} \text{ mol/l}$ and 30 min, respectively, silver nanoparticles with sizes of 8–10 nm in

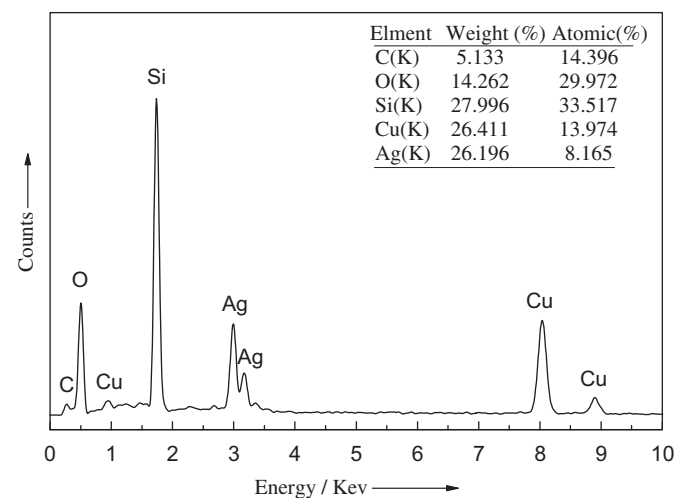


Fig. 3. EDX analysis of the silica spheres coated with a silver layer of 14 ± 2 nm in thickness.

diameter can be successfully deposited onto the surface of preformed colloidal silica spheres, [15] as is shown in Fig. 4a. However, when I is increased to 2.5 mA/cm^2 while the other conditions remain the same, it is observed that a consecutive silver layer consisting of nonuniform silver particles has formed and the surfaces of silver-coated silica spheres look rough, as shown in Fig. 4b. This may result from high growth rate of silver at a high current density. Moreover, when C is increased to $3.25 \times 10^{-4} \text{ mol/l}$ while the other conditions remain the same, the thickness of silver layer is up to about 20 nm, as that shown in Fig. 4c, the size distribution of silver nanoparticles gets wider and surface roughness increases. This is attributed to high growth rate of silver at a high concentration of the electrolyte. In addition, reaction time is a very important factor. For example, when reaction time is shortened to 15 min while other conditions remain the same, inhomogeneous silver nanoparticles formed on the surface of silica spheres. Thus, Ag distribution on silica spheres, e.g. the continuity, the surface roughness and the layer thickness, is controllable.

Some interesting information is obtained after comparison between the products shown in Figs. 1 and 4a. When I and C are relatively low, dispersive silver nanoparticles are formed, while continuous distribution of silver is observed when I and C increase to 2 mA/cm^2 and $3.25 \times 10^{-6} \text{ mol/l}$. However, when I and C exceed certain values (e.g., when I and C are, respectively, 3 mA/cm^2 and $6 \times 10^{-3} \text{ mol/l}$), no silver particles but large silver conglomerations form in the electrolyte. The effecting mechanisms of I and C are discussed respectively as follows. When I increases, more positive charges will aggregate on the silica surface and facilitate the nucleation to form a continuous silver layer. And the formation of the conglomerations in the electrolyte may result from the relatively strong electroreductive driving force for the ions at high I . And it is exactly the driving force that makes it difficult for silver ions to nucleate on silica spheres, because it makes the cathode more attractive than silica substrates. As for C , there exists a relatively larger radial concentration gradient near the silica spheres due to the larger concentration difference between the boundary layer and the electrolyte when C is low, which can promote the radial growth of the nuclei on the substrates. On the contrary, at high C , the concentration gradient becomes lower, which reduces the nuclei's

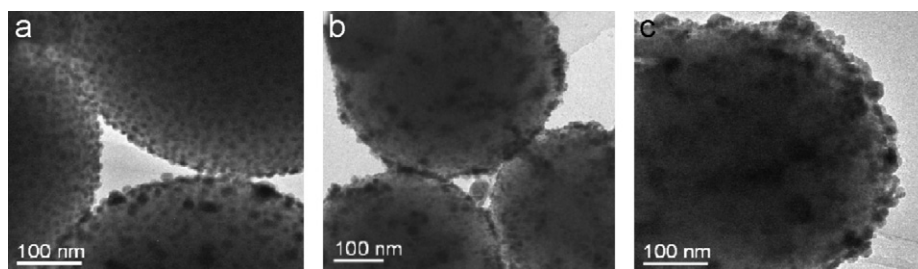


Fig. 4. TEM images of the samples synthesized when I , C and t are, respectively (a) 0.75 mA/cm^2 , $3.25 \times 10^{-7} \text{ mol/l}$ and 30 min; (b) 2.5 mA/cm^2 , $3.25 \times 10^{-6} \text{ mol/l}$ and 30 min; (c) 2.0 mA/cm^2 , $3.25 \times 10^{-4} \text{ mol/l}$ and 30 min.

tendency to grow radially, so the transverse growth becomes more apparent. The possible formation mechanism of the silica–silver core–shell composite particles is similar to that of ultrasonic electrodeposition of Ag nanoparticles on silica substrates [15]. That is silver ions in the electrolyte are bound to the surface of colloidal silica spheres to form a silver ion layer, due to the electrostatic interaction or possibly a moderately strong chemical bond ($\text{Si-O-Ag}^{\delta+}$) [17], then the silver ions bonded to the silica surface are reduced to form nucleating sites which then evolve into small nuclei. The nuclei act as suspensive nanoelectrodes and grow into silver nanocrystals with controllable continuity, surface roughness and layer thickness.

The modulation of the continuity of Ag distribution, the surface roughness and the thickness of silver layer makes it possible to improve the properties of the products. UV–visible spectroscopy was employed for further qualitative characterization of the optical properties of the materials. No visible peak appears in the spectrum of uncoated silica colloids (Fig. 5 curve a) because the dielectric function of silica is constant in the present wavelength range (300–800 nm). However, a weak broad peak appears at about 480 nm (Fig. 5 curve b) after the deposition of discrete silver nanoparticles of 8–10 nm (Fig. 4a). With increasing coating content (Fig. 2), an obvious and broad absorption peak appears at near 500 nm (Fig. 5 curve c), which is resulted from the coupling of the neighboring nanoparticles because the silver nanocrystals consecutively deposited on the silica surface may be considered as the “silver aggregates” [18,19]. This is consistent with the previous reports that the strong dipole–dipole interactions between neighboring nanoparti-

cles and Mie scattering of silver shell would promote redshift and broadening of the plasmon bands for silver clusters attached on silica spheres [9,20]. With an increase of the surface roughness and thickness of silver layer (Fig. 4c), the extinction band is broadened greatly and almost covers the wavelength range from 320 to 620 nm. In addition, one resonance band maximum and a minimum appears respectively at the wavelength of about 445 and 320 nm (Fig. 5 curve d), the minimum corresponds to a minimum in the imaginary part of the refractive index (about 0.4) for bulk silver [21]. The maximum band shifts to shorter wavelength comparing with curve b, which is consistent with previous literature reported by Halas’s group [22]. They have proposed that once the shell is complete, the peak absorbance is shifted to shorter wavelengths with the growth of gold shell.

4. Conclusions

In summary, silica–silver core–shell structure with a consecutive and uniform thin silver layer was successfully fabricated through a one-step ultrasonic electrodeposition method. The average single crystal size is about 12 nm and the thickness of silver consecutive layer is 14 ± 2 nm. Moreover, the continuity of Ag distribution, the surface roughness and the thickness of silver layer can be adjusted with the reaction conditions. With increasing coating content, the extinction band is broadened and red-shifted greatly. However, with an increase of the surface roughness and the thickness of silver layer, the more broadened extinction band is shifted to shorter wavelength. Such spheres provide promising applications, for example, in fabrication of metallic–dielectric PCs and providing new basic units for the construction of nanodevices for use in biochemical detection.

Acknowledgments

This research was supported by a grant for the State Key Program for Basic Research of China (Grant no. 2004CB619305), the National Natural Science Foundation of China (Grant no. 50571044, 50602022), and the Natural Science Foundation of Jiangsu Province (Grant no. BK2006716).

References

- [1] S. Nie, S.R. Emory, *Science* 275 (1997) 1102.
- [2] R.D. Averitt, S. Westcott, N.J. Halas, *J. Opt. Soc. Am.* 16 (1999) 1824.
- [3] Y. Lu, Y. Yin, Z.Y. Li, Y. Xia, *Nano Lett.* 2 (2002) 785.
- [4] C. Loo, A. Lowery, N. Halas, J. West, R. Drezek, *Nano Lett.* 5 (2005) 709.
- [5] S.I. Stoeva, F.W. Huo, J.S. Lee, C.A. Mirkin, *J. Am. Chem. Soc.* 127 (2005) 15362.
- [6] S. Phadtare, A. Kumar, V.P. Vinod, C. Dash, D.V. Palaskar, M. Rao, P.G. Shukla, S. Sivaram, M. Sastry, *Chem. Mater.* 15 (2003) 1944.
- [7] Z.L. Wang, C.T. Chan, W.Y. Zhang, N.B. Ming, P. Sheng, *Phys. Rev. B* 64 (2001) 113108.

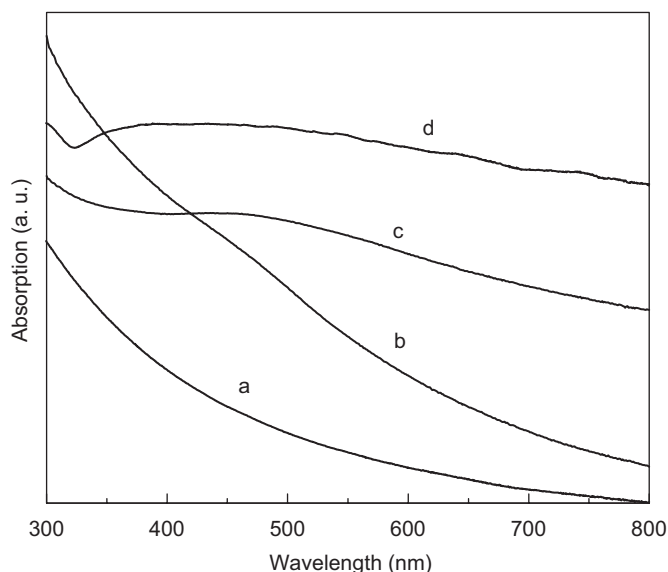


Fig. 5. UV–visible spectra of the silica colloids before and after deposition of silver nanocrystals (a) uncoated silica spheres; (b) silica spheres coated with uniform and isolated silver nanoparticles (as shown in Fig. 4a); (c) silica spheres coated with a silver layer of 14 ± 2 nm in thickness (as shown in Fig. 2); and (d) silica spheres coated with a silver layer of about 20 nm in thickness (as shown in Fig. 4c).

- [8] W.Y. Zhang, X.L. Lei, Z.L. Wang, D.G. Zheng, W.Y. Tam, C.T. Chan, P. Sheng, *Phys. Rev. Lett.* 84 (2000) 2853.
- [9] Y. Kobayashi, V. Salgueirinho-Maceira, L.M. Liz-Marzán, *Chem. Mater.* 13 (2001) 1630.
- [10] M.W. Zhu, G.D. Qian, Z.L. Hong, Z.Y. Wang, X.P. Fan, M.Q. Wang, *J. Phys. Chem. Solid.* 66 (2005) 748.
- [11] J.M. Lee, D.W. Kim, Y.H. Lee, S.G. Oh, *Chem. Lett.* 34 (2005) 928.
- [12] C. Graf, A. van Blaaderen, *Langmuir* 18 (2002) 524.
- [13] T. Cassagneau, F. Caruso, *Adv. Mater.* 14 (2002) 732.
- [14] A.B.R. Mayer, W. Grebner, R. Wannemacher, *J. Phys. Chem. B* 104 (2000) 7278.
- [15] S.C. Tang, Y.F. Tang, F. Gao, Z.G. Liu, X.K. Meng, *Nanotechnology* 18 (2007) 295607.
- [16] W. StÖber, A. Fink, E. Bohn, *J. Colloid Interface Sci.* 26 (1968) 62.
- [17] V.G. Pol, D.N. Srivastava, O. Palchik, V. Palchik, M.A. Slifkin, A.M. Weiss, A. Gedanken, *Langmuir* 18 (2002) 3352.
- [18] S.L. Westcott, S.J. Oldenburg, T.R. Lee, N.J. Halas, *Langmuir* 14 (1998) 5396.
- [19] S.L. Westcott, S.J. Oldenburg, T.R. Lee, N.J. Halas, *Chem. Phys. Lett.* 300 (1999) 651.
- [20] M.W. Zhu, G.D. Qian, G.J. Ding, Z.Y. Wang, M.Q. Wang, *Mater. Chem. Phys.* 96 (2006) 489.
- [21] P.B. Jonson, R.W. Christy, *Phys. Rev. Lett.* 6 (1972) 4370.
- [22] S.J. Oldenburg, R.D. Averitt, S.L. Westcott, N.J. Halas, *Chem. Phys. Lett.* 288 (1998) 243.